Structural, Optical and I-V Characteristics of ITO/p-Si Hetero-junction deposited by chemical Spray Pyrolysis

Salam Amir Yousif[1*] and Duha Ismail Khalil[1]

[1]*Physics Department, College of Education, Mustansiriyah University, Baghdad – Iraq.*

ABSTRACT

Indium Tin Oxide (ITO) thin films at different tin doping of 0, 5, 10, 15, and 20 wt% were successfully prepared using Chemical Spray Pyrolysis (CSP) method. The peaks of X-ray Diffraction (XRD) indicate that all samples have polycrystalline cubic structure and the plane (222) is the preferential orientation. AFM examinations show that the root means square roughness of ITO thin films decreased with increasing tin doping and the grain size transformed from microstructure to nanostructure when tin-doped with indium oxide. The maximum transmittance value measured is approximately 80% for the infrared region, and the bandgap is equal to 3.5, 3.7, 3.67, 3.65, and 3.58 eV corresponding to the concentration 0, 5, 10, 15, and 20%. The current-Voltage (I-V) characteristics of ITO/p-Si hetero-junction for dark and illuminated conditions have been investigated.

1. INTRODUCTION

Indium Tin Oxide (ITO) is an n-type transparent conducting oxides material. ITO has large optical transparency, low resistivity, energy bandgap larger than 3.5 eV, and it can be extensively applied in different technological applications such as antireflection coatings [1], solar cells [2, 3], liquid crystal displays [4], photocurrent generators [5], light-emitting diodes [6, 7] and gas sensors [8]. The ITO films are usually fabricated utilizing different methods like sputtering [9-11], sol-gel technique [12-14], vacuum thermal evaporation [15], pulsed laser deposition [16,17], chemical vapor deposition [18,19], and chemical spray pyrolysis [20-25].

Tirumoorthi and Prakash [26] prepared ITO thin films on a glass substrate using Chemical Spray Pyrolysis (CSP) method at different tin content. They showed that ITO films are polycrystalline cubic structure and they have detected a transfer of the preferential construction from [400] direction for un-doped films to [222] direction for doped films. The roughness and root mean square decreased with increased tin content and the optical transmittance was improved from 77% to 87%. The carrier concentration increased, the resistivity reduced and there is an improvement in the mobility when tin was doped in indium oxide. Yoo and Lee [27] studied the effect of annealing temperature on the electrical properties of ITO/n-type and p-type Si wafers Schottky junction using Rf magnetron sputtering technique. They found that a layer with positive charges was created between ITO film and silicon wafer and it can be removed (positive fixed charges) by heat treatment. The Schottky barrier of ITO/n-Si increased after annealing process and the barrier of ITO/p-Si decreased after the annealing process.

---

[*]Corresponding Author: *salammomica@yahoo.com*

This paper study the capability to prepare indium tin oxide thin films with high uniformity and good quality using the CSP method, and investigate the suitability of using ITO for optoelectronic application to produce ITO/p-Si photodetector.

2. EXPERIMENTAL PART

Indium tin oxide films at different tin doping were fabricated on glass slides at a substrate temperature about $(450 \pm 10)°C$ using the Chemical Spray Pyrolysis (CSP) technique as shown in Figure 1. Indium Chloride $InCl_3$ (98% purity, Thomas Baker, India), Stannic Chloride $SnCl_4.5H_2O$ (99% purity, Chemical Point, Germany), and distilled water were mixed thoroughly to obtain a sprayed solution with a concentration of 0.05 (mole/litre) and then hydrochloric (HCl) acid was added to the mixture to obtain a homogeneous and clear solution. Before deposition, glass substrates were cleaned ultrasonically in distilled water for 15 minutes and then the previous step was repeated with pure alcohol and pure acetone solution. The slides were desiccated via an air blower. The slides utilized for ITO/p-Si hetero-junction is mono-crystalline p-Si with the resistivity equal to (1.5-4) Ω. cm and $\langle 111 \rangle$ direction with a thickness equal to (508 ∓ 15) μm. Before the deposition process, Si slides were treated by the same above steps. One side of the Si surface was previously mechanically polished like a mirror. Native oxides were removed by 40:60 HF:H_2O solution. The size of a photodetector is 10×10 mm.
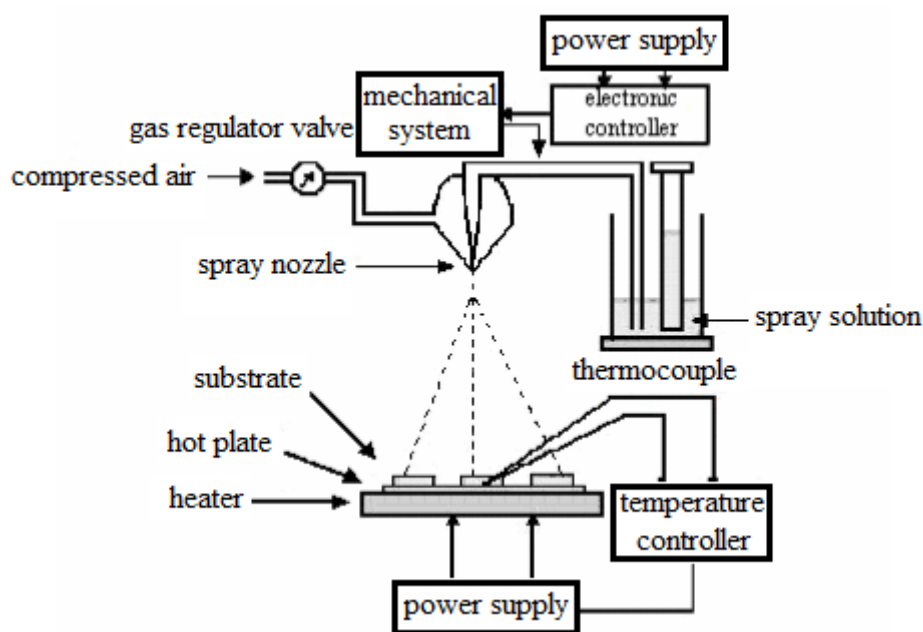

Figure 1. Graphical representation of CSP unit.

X-ray Diffraction (XRD) instrument which is Shimadzu 6000 was utilized to investigate the structural properties of the samples. Morphological parameters of the samples were examined employing (SPM AA3000 Angstrom Advanced Inc.). An ultraviolet-visible spectrophotometer (Shimadzu UV-1650 PC) was used to measure the optical parameters of ITO films from the transmittance and absorbance spectra at wavelength interval of 300 to 1000 nm. The current-voltage (I-V) characteristics of ITO/p-Si photodetector was tested successfully using the setup shown in Figure 2.
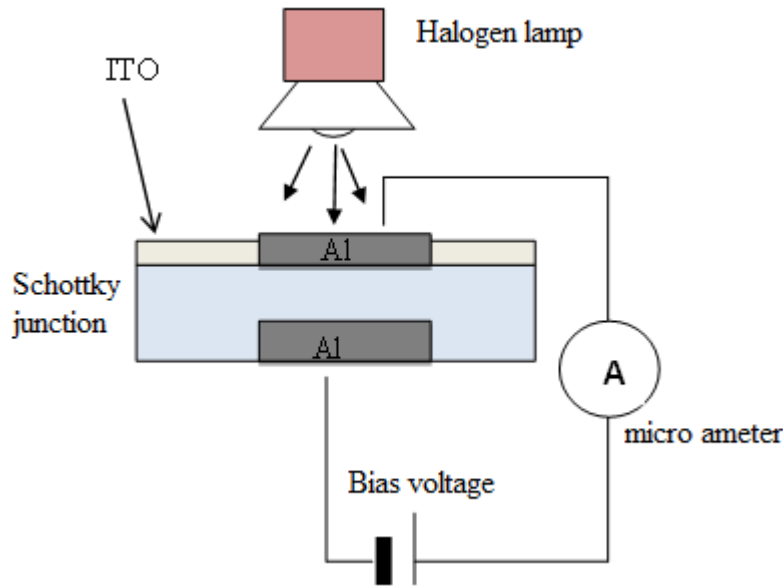
Figure 2. Schematic diagram of (I-V) characteristics setup.

3. RESULTS AND DISCUSSION

3.1 Structural Properties

Figure 3 illustrates the XRD pattern of indium tin oxide for various tin doping of 0, 5, 10, 15, and 20 wt% and was indexed with JCPDS (card 06-0416 $In_2O_3, cubic$). The presence of diffraction peaks indicates that the samples are polycrystalline cubic structure. The XRD measurements revealed that the In_2O_3 samples show a peak (400) as the highest intensity with a texture coefficient equal to 2.8418 as a preferred growth orientation, while the doped films have the peak (222) as the highest intensity. In other words, there is a shift in the construction direction from [400] to [222] when Sn was added to the In_2O_3. The transformation of preferential direction growth can be explained when tin atoms occupy vacant space in the indium. This result corresponds with another research [26]. The intensity of (222) peak rise with rising tin content in ITO samples and the intensity of (400) peak decreases with rising tin content in the samples. The rises of preferred direction growth are connected with the rises of the growth of crystallite film. The values of full width at half maximum (FWHM)(β), the lattice constant (a), the crystallite size (D), dislocation density (δ), strain ($\varepsilon_\circ$), and texture coefficient (TC) of ITO thin films were calculated employing the following theoretical equations and listed in Table 1.

The lattice parameter (a) of the cubic structure is given by:

$$a = \frac{d}{\sqrt{h^2+k^2+l^2}} \tag{1}$$

Where (d) is the spacing between planes and (hkl) is miller indices of that plane.

By using the Debye-Scherrer equation [28], the size of the crystallite (D) can be calculated as:

$$crystallite\ size\ (D) = \frac{0.9 \times wave\ length\ (\lambda)}{FWHM\ (\beta) \times cos\theta} \tag{2}$$

Where the wavelength of the incident x-ray beam ($\lambda = 1.5406$ Å), (β) is given (in radian) and finally (θ) represent the Bragg's angle (in degree).

Equation (3) and (4) were used to calculate the dislocation density (δ) and the strain ($\varepsilon_\circ$) [28]:

$$\delta = \frac{1}{D^2} \tag{3}$$

$$\varepsilon_\circ = \frac{\beta \cos\theta}{4} \tag{4}$$

Equation 5 shows the texture coefficient (TC) of the samples which explain the direction of preferential growth [29]:

$$T_c(hkl) = \frac{I(hkl)/I_0(hkl)}{N_r^{-1}\sum I(hkl)/I_0(hkl)} \tag{5}$$

Where $I(hkl)$ is the measured intensity, $I_0(hkl)$ is the standard intensity according to the JCPDS (card 06- 0416 $In_2O_3, cubic$) and N_r is the number of diffraction peaks presented.
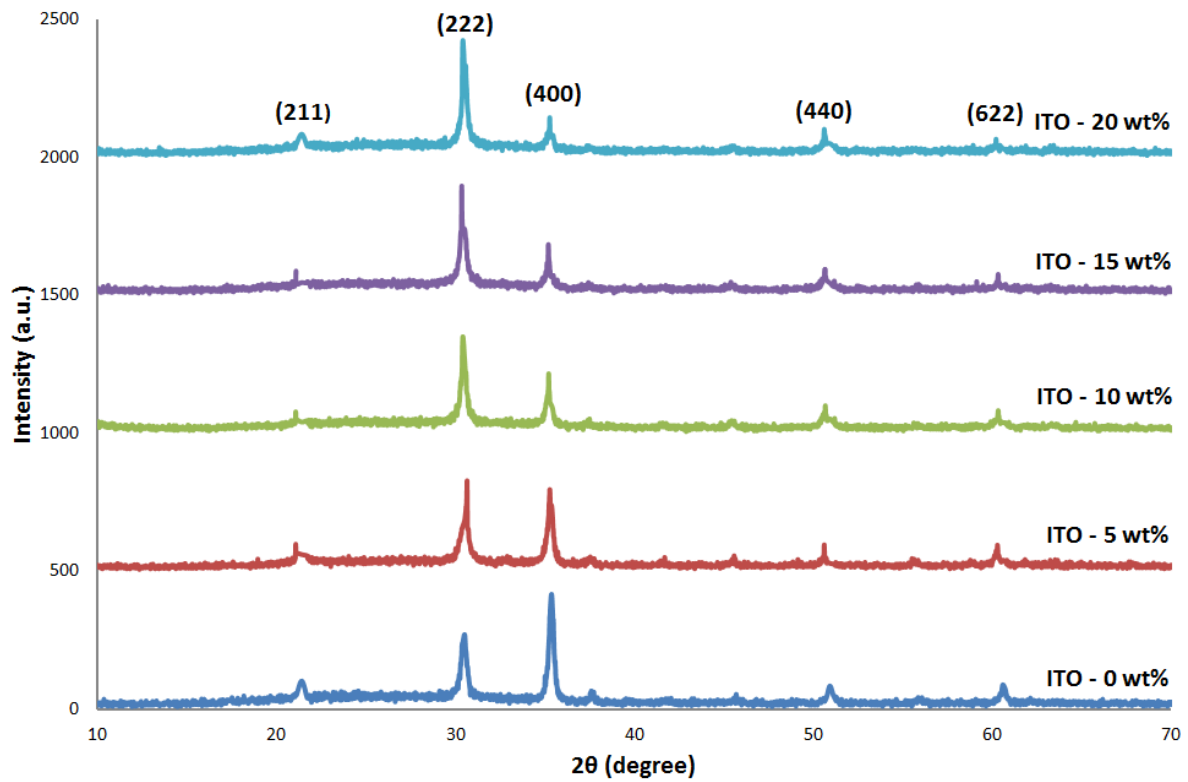

Figure 3. XRD pattern of ITO thin films at different tin doping.

In addition, Figure 3 shows a slight shift of (222) and (444) peaks across smaller angle (2θ) due to the alteration of tin ion in indium sites which cause the variation of strain in the lattice which corresponds with the report [30].

Table 1 Some structural parameters of $In_2O_3:Sn$ films

Tin-doping wt%	hkl	FWHM (deg)	D (nm)	δ line/m² (10¹⁵)	ε∘ (10⁻³)	Lattice parameter (Å)	texture coefficient (TC)
0	211	0.32000	25.2	1.57	1.37	10.16	0.6698
	222	0.33380	24.6	1.65	1.40	10.15	0.5285
	400	0.30140	27.6	1.31	1.25	10.14	2.8418
	440	0.27600	31.8	0.98	1.08	10.13	0.4140
	622	0.29470	31.2	1.02	1.11	10.12	0.5456
5	211	0.35500	22.7	1.94	1.52	10.15	0.7662
	222	0.40710	20.2	2.45	1.71	10.14	0.8252
	400	0.35480	23.5	1.81	1.47	10.13	2.1730
	440	0.41330	21.2	2.22	1.62	10.13	0.5422
	622	0.40170	22.9	1.90	1.51	10.12	0.6931
10	211	0.36000	22.4	1.99	1.54	10.16	0.8218
	222	0.40180	20.4	2.40	1.69	10.15	1.0460
	400	0.36670	22.7	1.94	1.52	10.14	1.6736
	440	0.35600	24.7	1.63	1.40	10.13	0.7471
	622	0.39500	23.2	1.85	1.48	10.13	0.7112
15	211	0.35340	22.8	1.92	1.51	10.18	0.7889
	222	0.40600	20.2	2.45	1.70	10.16	1.1045
	400	0.34760	23.9	1.75	1.44	10.15	1.7304
	440	0.41330	21.2	2.22	1.62	10.14	0.7574
	622	0.40600	22.6	1.95	1.53	10.14	0.6185
20	211	0.32660	24.7	1.63	1.40	10.15	0.8568
	222	0.36850	22.3	2.01	1.55	10.14	1.3328
	400	0.35130	23.7	1.78	1.46	10.14	1.3328
	440	0.46500	18.9	2.79	1.83	10.13	0.8377
	622	0.53500	17.1	3.41	2.01	10.13	0.6397

3.2   Topography Properties

Three-dimensional AFM pictures of $In_2O_3:Sn$ samples at various tin doping are illustrated in Figure 4. Table 2 shows that the AFM parameters are varied with rising tin doping. The roughness of ITO samples decreases from 4.68 to 2 nm with rising tin content in the samples due to lower vacancy defects and the rearrangement of atoms in the samples. The morphological measurements show that the samples have high uniformity surface and such surface can be used in solar cells or photodetector.

The grain size (D) values of ITO samples are 107, 95, 96, 100, and 77 nm for tin content 0, 5, 10, 15, and 20 wt%, respectively. The size of the grains transformed from microstructure to nanostructure when tin was doped with indium oxide. AFM study reveals that the grain size and the surface roughness of ITO samples are strongly dependent on the concentration of the tin content in the samples.
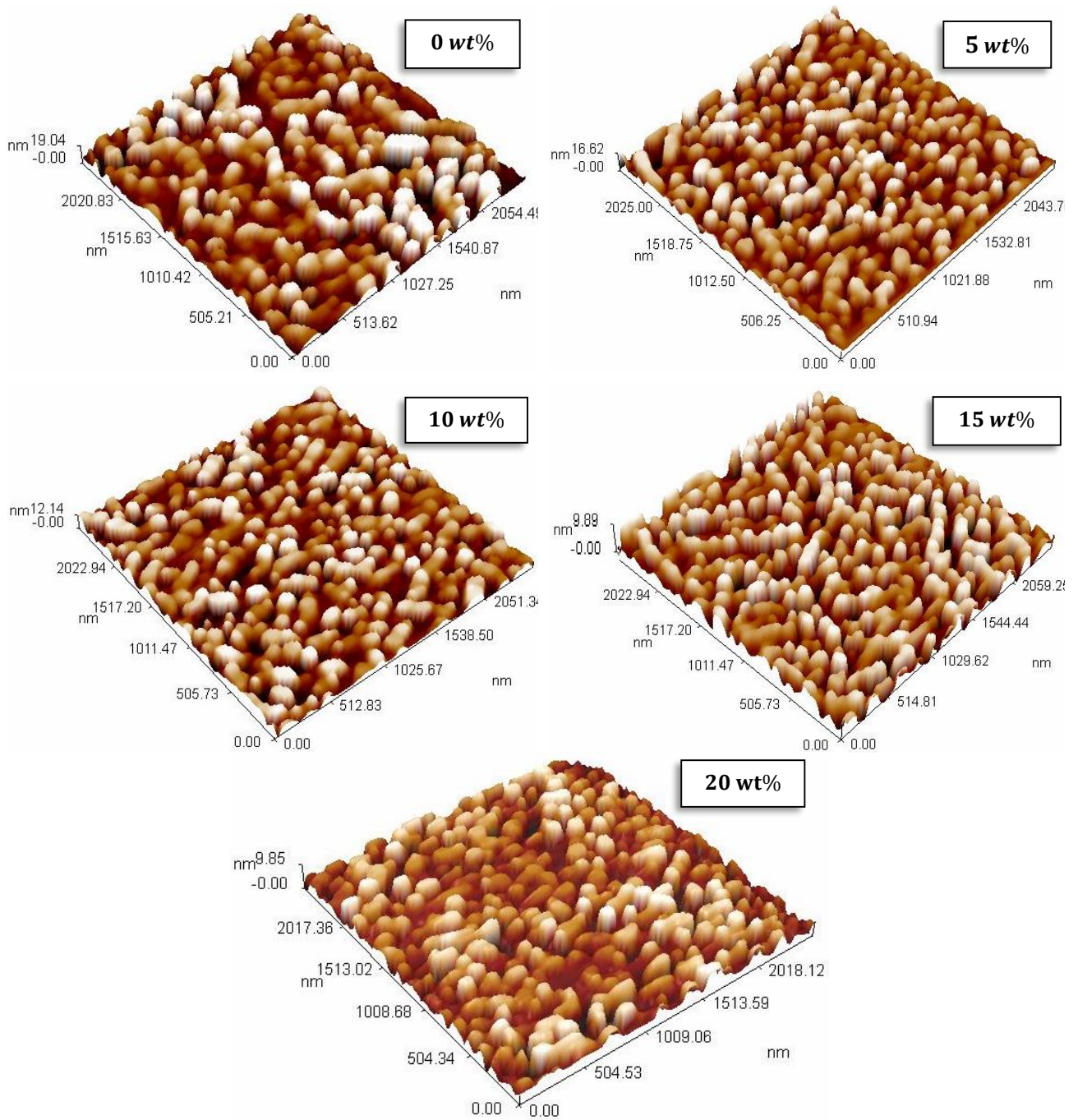
Figure 4. AFM images of ITO thin films at different tin doping.

Table 2 Morphological parameters of ITO films

Tin content	Root Mean Square roughness (nm)	Gain size (nm)
0 wt%	4.68	107
5 wt%	3.56	95
10 wt%	2.75	96
15 wt%	2.3	100
20 wt%	2	77

3.3   Optical Properties

The transmittance and absorbance spectrum of ITO samples were calculated at 27°C in the range from 300 nm to 1000 nm. Figure 5 shows that the transmittance of ITO samples rises with rising tin concentration up to 5%. Thereafter, it goes on decreases gradually with rising tin concentration at 10, 15, 20%. The transmittance of ITO samples decreases after the addition of a large amount of impurity which increases the scattering of photons resulted from crystal defects (impurities), which is compatible with report [31]. Figure 6 illustrates the absorbance curves of ITO films as a function of the calculated wavelength.
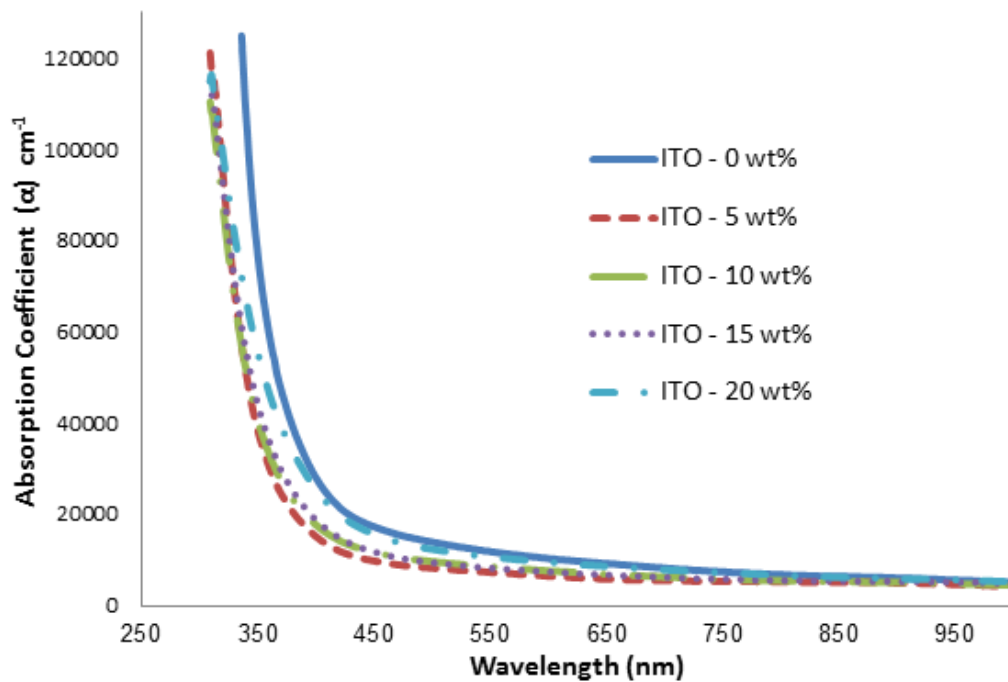

Figure 5. Transmittance spectra of ITO thin films.

Figure 6. The absorption coefficient of ITO thin films.

Equation (6) shows the relation of absorption coefficient and photon energy (hγ) for direct transition [28]:

$$\alpha h\gamma = A(h\gamma - E_g)^X \tag{6}$$

Where (hγ) is the photon energy, (E_g) is the energy band gap and (A) is constant.

The optical band gap of ITO thin films is found to be 3.5, 3.7, 3.675, 3.65, and 3.58 eV corresponding to the tin content (refer Figure (7)). In Figure (8), the optical band gap of ITO samples rises with rising tin content up to 5%, due to the rises of carrier density with rising tin content. then its reduction for further rising in tin content from 5 to 20%, this behaviour can be explained by the formation of donor levels near the conduction band in the energy gap caused by the impurities that absorb low energy photons [32].
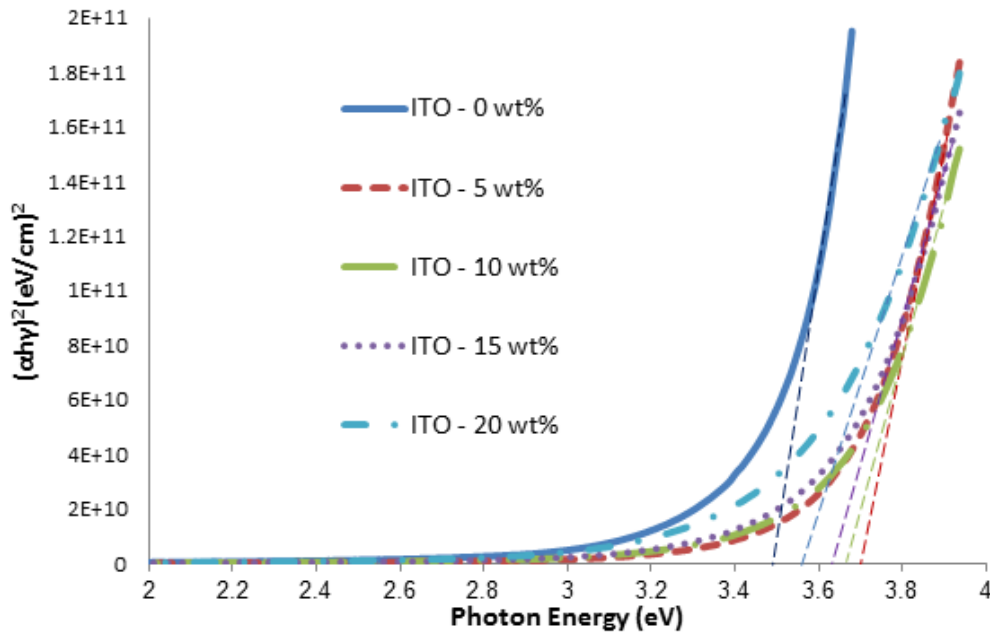
Figure 7. Variation of $(\alpha h\gamma)^2$ vs. photon energy $(h\gamma)$ for ITO thin films at different tin doping.
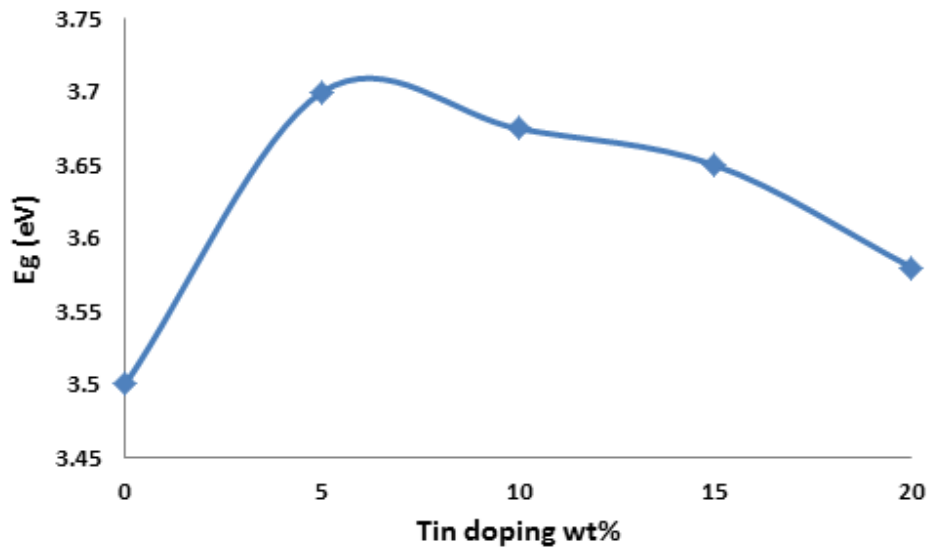
Figure 8. The energy bandgap (E_g) of ITO thin films as a function of tin doping.

3.4 I-V Characteristics

I-V characteristics of ITO/p-Si heterojunction were investigated under dark conditions as shown in Figure (9). In practice, the diode does not exactly obey the theoretical diode relation. The ideality factor (B) can be calculated using the following equation and listed in Table (3):

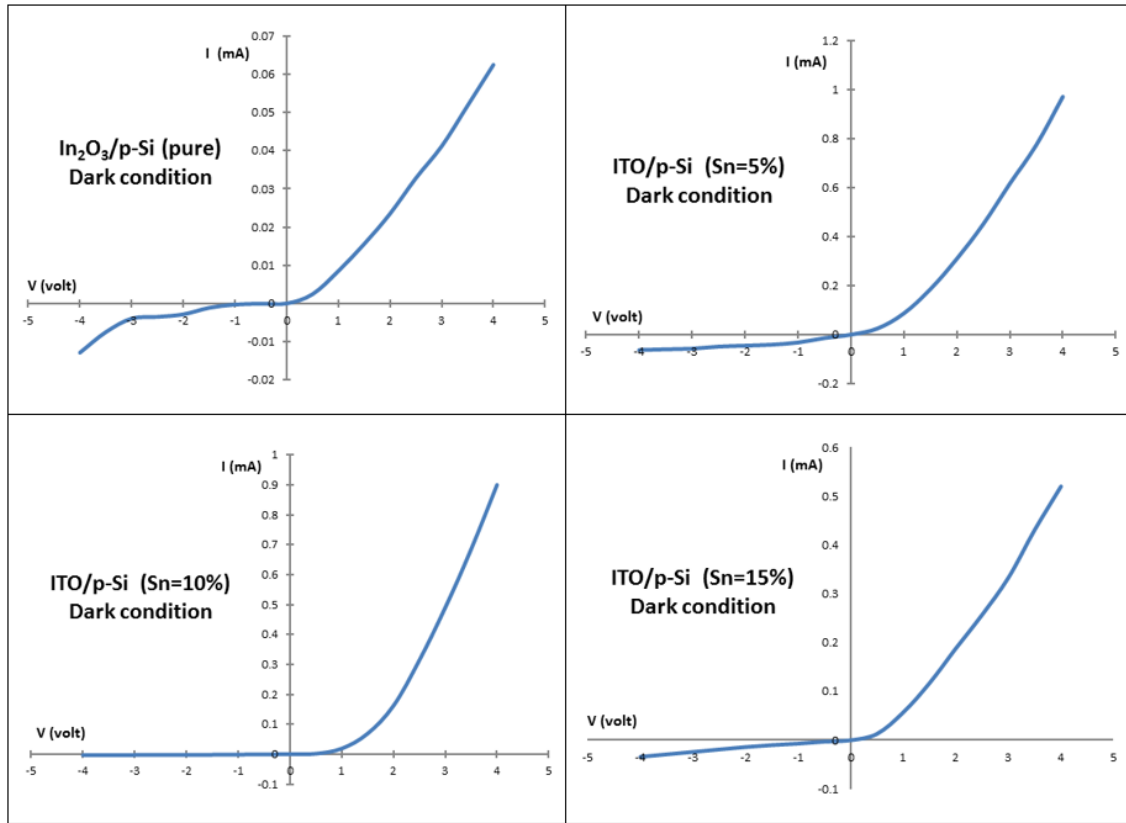$$B = \frac{q}{K_B T} \frac{V}{ln\frac{I}{I_s}}$$
(7)

Where: V is the forward bias voltage, K_B is Boltzmann constant and I_s is the saturation current.

It is known that the reverse bias current increased after illuminating the ITO/p-Si junction due to the electron-hole pairs created in the depletion region if the energy of the incident photon is greater than the direct energy bandgap of the ITO/p-Si hetero-junction. Figure (10) shows a current-voltage relation of ITO/p-Si hetero-junction for murky and shining conditions at reverse bias.

Where the current under murky condition can be noted by (I_d), the current under shining condition can be noted by (I_t), therefore, the photocurrent is given by Equation (8):

$$(I_{ph} = I_t - I_d)$$
(8)

it can be seen clearly that the photocurrent (I_{ph}) rise with rising tin content up to 5%, then it reduce when there is further rising of tin content in the samples due to the optical bandgap of the films rise with rising tin content up to 5% and then begin to decreases with the rising tin content in the films.
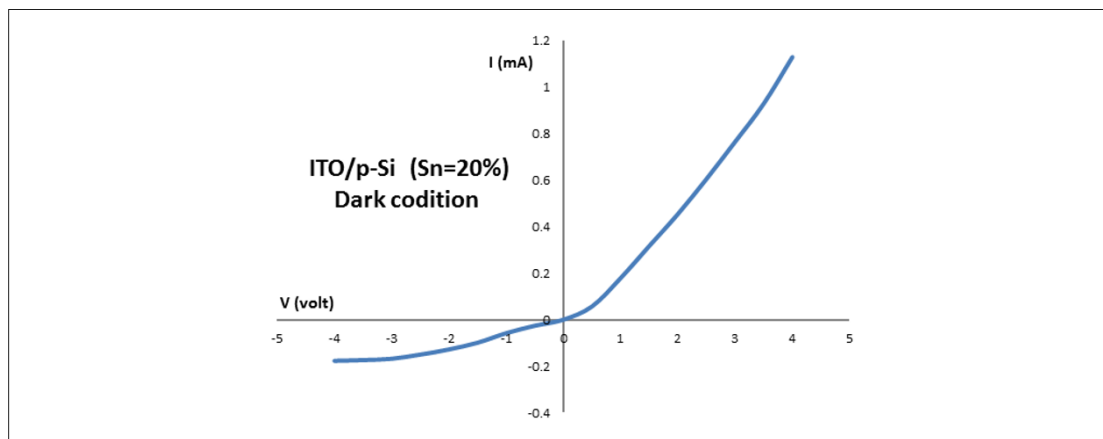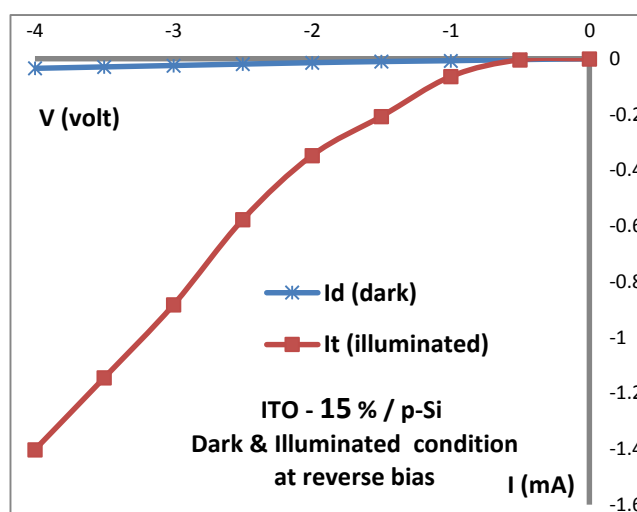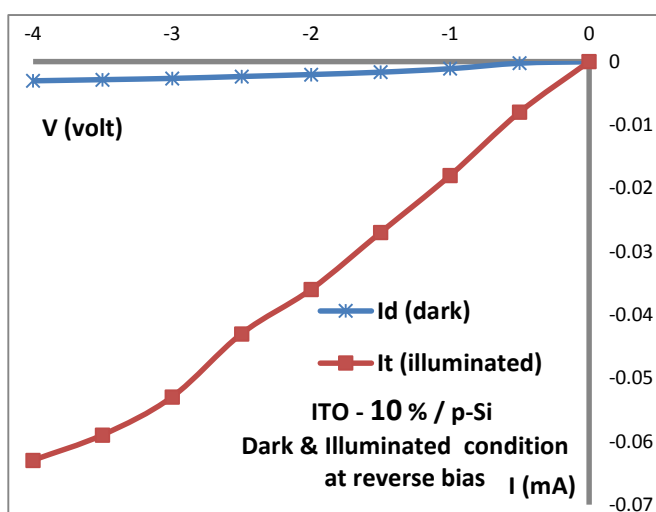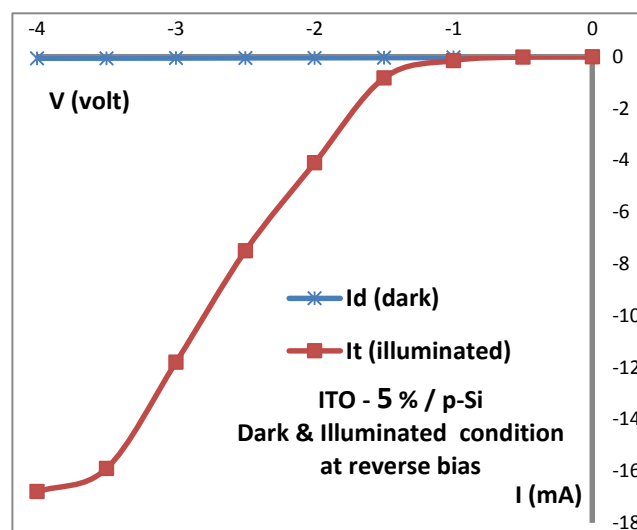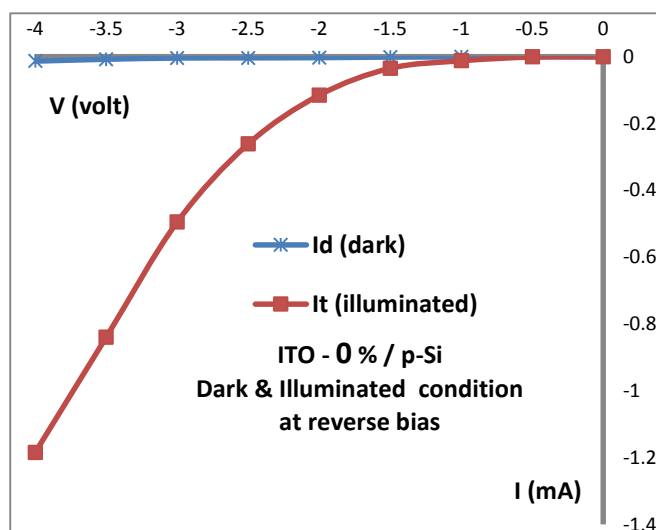
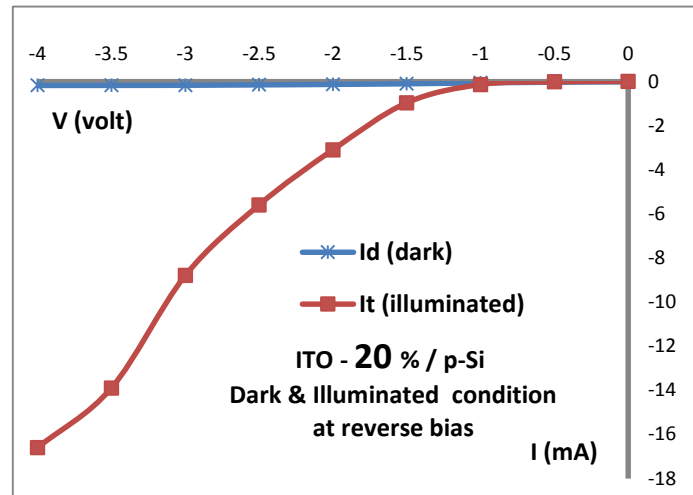**Figure 9.** I-V curve of ITO/p-Si Heterojunction under dark condition.

Figure 10. I-V curve of ITO/p-Si hetero-junction under the dark and illuminated condition at reverse bias voltage.

The spectral response of ITO/p-Si hetero-junction for white light was calculated using the following equation and listed in Table (3):

$$R_\lambda = \frac{I_{ph}}{P_{in}} \ (A/W)$$ (9)

Where: I_{ph} is the photocurrent and P_{in} is the input power.

Table 3 Ideality factor and Spectral response of ITO/p-Si hetero-junction

Sn – content wt%	Ideality Factor (B)	Spectral Response (A/W) at 550 nm
0	6.63	1.1215
5	4	4.055
10	1.7	3.396
15	2.9	3.33
20	6.1	2.972

From current-voltage characteristics of ITO/p-Si heterojunction, the result suggests that $In_2O_3:Sn$ film deposited by chemical spray pyrolysis method is suitable for optoelectronic application such as solar cells and photodetectors.

4. CONCLUSION

Indium Tin Oxide (ITO) thin film was successfully prepared on glass and p-type silicon substrates by CSP method. The effect of tin concentration on the structural, morphological, optical and I-V characteristic of ITO/p-Si heterojunction was investigated. This study concludes that there is a shift in the construction direction from [400] to [222] direction when Sn was added to the In_2O_3 hence, confirms the substitution of tin in the indium-oxide lattice. The RMS roughness values decreased with rising tin doping concentration and the grain size transformed

from microstructure to nanostructure when tin was doped with indium oxide. The optical band gap rises from 3.5 eV at (0 wt%) to 3.7 eV at (5 wt%) and then decreased to 3.58 eV at (20 wt%). The rises in optical bandgap with rising carrier concentration are explained by applied Moss-Burstein theory. The reducing of energy bandgap for larger tin content concentration is due to the effects of interaction through free carriers and ionized impurities or through free carriers. From the results in this research, it can be deduced that indium tin oxide films can be manufactured through Chemical Spray Pyrolysis (CSP) method with uniform, homogeneous and good quality films. ITO thin films are appropriate for optoelectronic application especially for ITO/p-Si photo-detector.

REFERENCES

[1]   S. A. Yousif, H. G. Rashid, K. A. Mishjil & N. F. Habubi, "Design and Preparation of Low Absorbing Antireflection Coatings Using Chemical Spray Pyrolysis" International Journal of Nanoelectronics and Materials **11**, 4, (2018) 449-460.

[2]   K. Yamamoto, M. Yoshimi, Y. Tawada, Y. Okamoto, A. Nakajima & S. Igari, "Thin-film poly-Si solar cells on glass substrate fabricated at low temperature", Appl. Phys. A **69** (1999) 179-185.

[3]   D. Gebeyehu, C. J. Brabec, N. S. Sariciftci, D. Vangeneugden, R. Kiebooms, D. Vanderzande, F. Kienberger & H. Schindler, "Hybrid solar cells based on dye-sensitized nanoporous TiO_2 electrodes and conjugated polymers as hole transport materials" Synth. Met. **125** (2001) 279-287.

[4]   J. C. Manifacier, "Thin metallic oxides as transparent conductors", Thin Solid Films **90** (1982) 297-308.

[5]   W. J. Lee, R. S. Mane, S. H. Lee & S. H. Han, "Enhanced photocurrent generations in $RuL_2(NCS)_2$/di-(3-aminopropyl)-viologen self-assembled on In_2O_3 nanorods", Electrochem. Commun. **9** (2007) 1502-1507.

[6]   S. T. Lee, Z. Q. Gao & L. S. Hung, "Metal diffusion from electrodes in organic light-emitting diodes", Appl. Phys. Lett. **75** (1999) 1404.

[7]   H. Kim, C. M. Gilmore, A. Pique, J. S. Horwitz, H. Mattoussi, H. Murata, Z. H. Kafafi & D. B. Chrisey, "Electrical, optical, and structural properties of indium–tin–oxide thin films for organic light-emitting devices", J. Appl. Phys. **86** (1999) 6451.

[8]   N. G. Patel, P. D. Patel, V. S. Vaishnav, "Indium tin oxide (ITO) thin film gas sensor for detection of methanol at room temperature", Sensors and Actuators B: Chemical **96** (2003) 180-189.

[9]   J. H. Park, C. Buurma, S. Sivananthan, R. Kodama, W. Gao & T. A. Gessert, "The effect of post-annealing on Indium Tin Oxide thin films by magnetron sputtering method" Appl. Surf. Sci. **307** (2014) 288-392.

[10]   L. Dong, G. Zhu, H. Xu, X. Jiang, X. Zhang, Y. Zhao, D. Yan, L. Yuan and A. Yu," Fabrication of Nanopillar Crystalline ITO Thin Films with High Transmittance and IR Reflectance by RF Magnetron Sputtering" Materials **12** (2019) 958.

[11]   K. C. Heo, Y. K. Sohn & J. S. Gwag, "Effects of an additional magnetic field in ITO thin film deposition by magnetron sputtering" Ceram. Int. **41** (2015) 617-621.

[12]   Y. Wang, J. Liu, X. Wu & B. Yang, "Adhesion enhancement of indium tin oxide (ITO) coated quartz optical fibers" Appl. Surf. Sci. **308** (2014) 341-346.

[13] M. T. Kesim & C. Durucan, "Indium tin oxide thin films elaborated by sol-gel routes: The effect of oxalic acid addition on optoelectronic properties" Thin Solid Films **545** (2013) 56-63.

[14] L. Korosi, S. Korosi & I. Dekany, "Preparation of transparent conductive indium tin oxide thin films from nanocrystalline indium tin hydroxide by dip-coating method" Thin Solid Films **519** (2011) 3113-3118.

[15] K. -Y. Pan, L. -D. Lin, L. -W. Chang & H. C. Shih, "Studies on the optoelectronic properties of the thermally evaporated tin-doped indium oxide nanostructures" Appl. Surf. Sci. **273** (2013) 12-18.

[16] J. B. Choi, J. H. Kim, K. A. Jeon & S. Y. Lee, " Properties of ITO films on glass fabricated by pulsed laser deposition" Mater. Sci. Eng. **102** (2003) 376-379.

[17] J. M. Dekkers, G. Rijnders & D.H. A. Blank, "Role of Sn doping in In_2O_3 thin films on polymer substrates by pulsed-laser deposition at room temperature" Appl. Phys. Lett. **88** (2006) 151908.

[18] Y. C. Park, Y. S. Kim, H. K. Seo, S. G. Ansari & H. S. Shin, "ITO thin films deposited at different oxygen flow rates on Si(100) using the PEMOCVD method" Surf. Coat. Technol. **161** (2002) 62-69.

[19] Y. S. Kim, Y. C. Park, S. G. Ansari, B. S. Lee & H. S. Shin, "Effect of substrate temperature on the bonded states of indium tin oxide thin films deposited by plasma enhanced chemical vapor deposition" Thin Solid Films **426** (2003) 124-131.

[20] G.G. Untila, T.N. Kost, A.B. Chebotareva, "Fluorine- and tin-doped indium oxide films grown by ultrasonic spray pyrolysis: Characterization and application in bifacial silicon concentrator solar cells" Solar Energy **159** (2018) 173–185.

[21] R. Rana, J. Chakraborty, S. K. Tripathi, M. Nasim**, "**Study of conducting ITO thin film deposition on flexible polyimide substrate using spray pyrolysis**"** J Nanostruct Chem **6** (2016) 65–74.

[22] K. Navya, S. P. Bharath, K. V. Bangera, G. K. Shivakumar, "Effect of indium content on the characteristics of indium tin oxide thin films" Mater. Res. Express **5** (2018) 096410.

[23] L. Zhang, J. Lan, J. Yang, S. Guo, J. Peng, L. Zhang, S. Tian, S. Ju, W. Xie, "Study on the physical properties of indium tin oxide thin films deposited by microwave-assisted spray pyrolysis "Journal of Alloys and Compounds **728** (2017) 1338-1345.

[24] A. R. Babar, S. S. Shinde, A. V. Moholkar, C. H. Bhosale, J. H. Kim & K. Y. Rajpure, "Sensing properties of sprayed antimony doped tin oxide thin films: Solution molarity" J. Alloys Compd. **509** (2011) 3108-3115.

[25] K. Ravichandran and K. Thirumurugan, "Type Inversion and Certain Physical Properties of Spray Pyrolysed SnO_2:Al Films for Novel Transparent Electronics Applications"J. Mater. Sci. Technol. **30** (2014) 97-102.

[26] M. Thirumoorthi & J. Thomas Joseph Prakash, "Structural, optical and electrical properties of indium tin oxide ultra-thin film prepared by jet nebulizer spray pyrolysis technique", Journal of Asian Ceramic Societies **4** (2016) 124-132.

[27] Keon Yoo, and Jong-Ho Lee, "Effect of Low Temperature Annealing on ITO-on-Si Schottky Junction" IEEE Electron Device Letters **38** (2017) 426-429.

[28] M. Thirumoorthi & J. Thomas Joseph Prakash," Structural, morphological characteristics and optical properties of Y doped ZnO thin films by sol-gel spin coating method" Superlattices and Microstructures **85** (2015) 237-247.

[29] S. S. Shinde, P. S. Shinde, S. M. Pawar, A. V. Moholkar, C. H. Bhosale & K. Y. Rajpure, "Studies on pure and fluorine doped vanadium pentoxide thin films deposited by spray pyrolysis technique" Solid State Sci. **10** (2008) 1209-1214.

[30] G. B. Gonzalez, J. B. Cohen, J. H. Hwang, T. O. Mason, J. P. Hodges & J. D. Jorgensen, "Neutron diffraction study on the defect structure of indium-tin-oxide", J. Appl. Phys. **89** (2001) 2550-2555.

[31] A. H. Al-Hamdani, ''Structural and Optoelectronic Properties of Nanostructured ITO Thin Films Deposited by Chemical Spray Pyrolysis Technique'', Journal of Materials Science and Engineering **12** (2014) 346-352.

[32]   S. D. M AL-Algawi, S. H Al-Jawad & N. M. Saadoon, "Physical Properties of Indium Tin Oxide (ITO) Nanoparticle Thin Films Used as Gas Sensor", Eng. &Tech. Journal **33** (2015) 141-15.